

# Energy Migration in the Aromatic Vinyl Polymers. 1. A One-Dimensional Random Walk Model

Patrick D. Fitzgibbon<sup>†</sup> and Curtis W. Frank\*

Department of Chemical Engineering, Stanford University, Stanford, California 94305.  
Received October 8, 1981

**ABSTRACT:** A strictly one-dimensional random walk model is developed to describe singlet exciton migration in isolated chains of the aromatic vinyl polymers. The polymer chain is considered to contain two types of sites: traps consisting of trans,trans meso dyads which can lead to excimer fluorescence and nontraps consisting of single repeat units or monomer sites. The model successfully explains the molecular weight dependence of intramolecular excimer fluorescence from poly(2-vinylnaphthalene) in a dilute solution of 2-methyltetrahydrofuran at low temperature.

## Introduction

The photophysics of the aromatic vinyl polymers, in particular the phenomenon of energy migration, has been a topic of study for the past 2 decades. Although questions have been raised recently,<sup>1</sup> Klöpffer has shown in a recent review<sup>2</sup> that singlet energy migration is a property of most aromatic polymers. In general, energy migration among the pendant aromatic rings is assumed to be a random process. There is a finite probability at every step in the walk that the excitation can be emitted as monomer fluorescence, dissipated by nonradiative processes, or transferred to another aromatic ring. In representative experiments which demonstrate the existence of energy migration, it has been found that impurity quenching<sup>3-5</sup> and the amount of excimer fluorescence<sup>6,7</sup> are larger than can be explained in its absence.

One approach to the determination of the contribution of energy migration to the photophysical behavior is to study the molecular weight dependence of excimer fluorescence. In previous work on naphthyl-containing polymers Nishijima has examined poly(1-vinylnaphthalene) (P1VN) in methylene chloride solution<sup>8</sup> and poly(2-vinylnaphthalene) (P2VN) both in 2-methyltetrahydrofuran solution<sup>9</sup> and in a glassy polystyrene (PS) matrix.<sup>10</sup>

The present work is the first in a series of studies on energy migration in the aromatic vinyl polymers. In this paper a one-dimensional model for the energy migration is developed and applied to the molecular weight dependence of P2VN in 2-methyltetrahydrofuran and toluene solution. In the following paper, it is applied to PS in rubbery miscible blends with poly(vinyl methyl ether).

The use of excimer fluorescence as a probe of energy migration in solutions of the aromatic vinyl polymers is complicated by the fact that the trap sites are not fixed. Although the overall concentration of excimer-forming sites (EFS) should be constant at equilibrium for a given temperature, the specific dyad states of a particular sequence in the chain backbone will be changing constantly due to segmental rotation. Whether this is significant or not depends upon the relative rates of migration and rotational motion.

If the rate of energy migration is fast relative to the rate of segmental rotation, the EFS trap distribution over a restricted length of the polymer chain will be fixed. As such, the identity of a particular dyad will not change during the sampling lifetime of a random walker. On the other hand, if the rate of segmental motion is much faster than exciton hopping, the identity of a particular dyad

would be different for subsequent sampling during a random walk.

The model developed in this paper treats only the first case for which energy migration is facile relative to segmental motion. In the model, the exciton motion is assumed to consist entirely of nearest-neighbor hops along the polymer chain. Since it is further assumed that the migrating excitation energy cannot hop past an EFS trap, these traps will serve to subdivide the polymer chain into a series of various length nontrap sequences. As such, the process is modeled as a one-dimensional random walk on a finite-length region. The analysis of the molecular weight dependence of excimer fluorescence then reduces to a consideration of the distribution of nontrap sequences in a given polymer and the relative probabilities of excimer and monomer emission from each such sequence. The objective of the study is to determine both the probability of emission at each step and the effective EFS concentration from the dependence of the relative excimer fluorescence on the molecular weight.

## Development of Model

**1. Background.** The mathematical analysis is based on the randomness of the hopping process. An excellent monograph that reviews the theory and applications of random and restricted walks to polymers is available.<sup>11</sup> In work relevant to this study, Rosenstock<sup>12</sup> considered a random walk on one-, two-, and three-dimensional lattices with traps at all boundaries and a finite probability,  $\alpha$ , of emission from the lattice at each hop. In his analysis, he determined the limiting behavior as  $\alpha$  approaches zero for an infinitely long chain. Levinson<sup>13</sup> considered the same problem but took an alternate approach to the construction of the difference equation. He determined the limiting probability of eventual monomer emission for a one-dimensional random walk on an infinite lattice on which quenchers were randomly distributed with concentration  $q$ . His limiting expressions were developed by allowing  $\alpha$  and  $q$  to approach zero in a manner such that  $q(2/\alpha)^{1/2}$  remained constant.

Statistical analysis of the random nature of energy migration has been applied to photophysical experiments by several authors. Klöpffer<sup>14</sup> applied the formalism of Rosenstock<sup>12</sup> and Rudemo<sup>15</sup> to excimer fluorescence of neat poly(*N*-vinylcarbazole) (PVK) films and determined that the concentration of traps due to excimer-forming sites was  $10^{-3}$  and that the average number of exciton hops was  $10^3$ . Dale and Eisinger<sup>16</sup> have discussed using this formalism to determine macromolecular dimensions and conformational dynamics from the concentration dependence of quenching. This model has also been used to examine the effect of tacticity on excimer fluorescence from poly(*p*-methylstyrene)<sup>17</sup> and poly(naphthyl methacrylate).<sup>18</sup>

<sup>†</sup> Presently at E. I. du Pont de Nemours and Co., Inc., Polymer Products Department, Experimental Station, Wilmington, Del.

If the singlet energy is assumed to migrate down the polymer chain by a series of random walk steps, each occurring with a probability given by the Förster expression,<sup>19</sup> a migration coefficient,  $\Lambda$ , may be defined by<sup>6</sup>

$$\frac{2\Lambda}{r^2} = \frac{1}{\tau} \left( \frac{R_0}{r} \right)^6 \quad (1)$$

in which  $r$  is the mean separation between chain neighbors,  $\tau$  is the fluorescence lifetime in the absence of transfer, and  $R_0$  is the Förster radius at which emission and transfer are equally likely.

Finite values of  $\Lambda$  have been obtained by application of this analysis to fluorescence quenching of P2VN, PVK, and vinylcarbazole-methyl methacrylate copolymers by North and Treadaway<sup>6</sup> and to quenching of PS of various molecular weights by Ishii.<sup>20</sup> In the recent work of Webber,<sup>21</sup> however,  $\Lambda$  for P2VN was concluded to be zero, within experimental accuracy. In this paper, we show that energy migration is required in order to explain the molecular weight dependence of excimer formation in P2VN.

**2. Assumptions.** The polymer molecule is assumed to consist of two types of sites distributed randomly along the chain: EFS traps and nontraps consisting of single repeat units or "monomer" sites. Nonadjacent intramolecular and intermolecular excimers are excluded; excimers are considered to consist only of complexes formed between aromatic rings which are in adjacent positions on the chain. The EFS traps are in small concentration; the bulk of the chain consists of nontrap sequences of monomer sites.

The exciton is modeled as a particle executing a symmetric one-dimensional Markoffian random walk on a region which has the same number of sites as the polymer molecule has monomer segments. Although it is possible to incorporate variable step lengths into the random walk,<sup>22</sup> only nearest-neighbor transfers are considered here. The exciton is assumed to have an equal probability of beginning at any site on the chain. All time intervals between hops are assumed equal to the average time between hops. At any hop, the exciton has a constant probability,  $\alpha$ , of being emitted instead of hopping to a neighboring site;  $\alpha$  is assumed to be independent of molecular weight. The probability that this emission will be radiative rather than nonradiative,  $Q_M$ , is assumed constant in space and time and equal to that of the monomeric model compound. The excimer quantum yield,  $Q_D$ , is also assumed to be constant.

**3. Probability of Eventual Monomer Emission.** At a monomer (nontrap) site the exciton has three options; it could either hop right or left one unit, or the energy could be dissipated. The dissipation could take the form of an emitted photon or it could consist of vibrational energy which would quickly degrade to thermal energy. The difference equation which describes this situation is  $F(m, k) =$

$$\alpha + \frac{1}{2}(1 - \alpha)F(m, k - 1) + \frac{1}{2}(1 - \alpha)F(m, k + 1) \quad (2)$$

where  $\alpha$  is the probability that the energy is emitted radiatively or nonradiatively and  $F(m, k)$  is the probability that an exciton starting a distance  $k$  units from the start of a sequence of  $m$  consecutive nontrap sites will eventually be emitted from a monomer site. The difference equation was solved by Levinson,<sup>13</sup> who found that

$$F(m, k) = 1 + C_1 e^{2\gamma k} + C_2 e^{-2\gamma k} \quad (3)$$

where

$$\gamma = \frac{1}{2} \ln \left[ \frac{1 + (2\alpha - \alpha^2)^{1/2}}{1 - \alpha} \right] \quad (4)$$

In order to evaluate the constants in eq 3, boundary conditions must be specified. Since the sequence of nontrap units could be terminated at boundaries consisting of either chain ends or traps, three situations may be distinguished. First, if there are no traps on the chain, the sequence of monomer sites would be terminated by the physical chain ends (case A). Alternatively, one terminus of the sequence could be a trap and the other could be the chain end (case B). Finally, the sequence could be terminated at both ends by traps (case C).

The exciton behavior at the chain end is governed by the elastic constant  $\beta$ , which represents the fraction of the time that the exciton will be reflected at the boundary. If the terminal repeat unit has the same probability for excimer formation as the interior units,  $\beta$  will be unity. In other words, an exciton attempting to hop off the chain will remain at the chain end. If, on the other hand, the chain is in dilute solution and the steric hindrance is sufficiently reduced at the chain end to promote greater segmental mobility, there may be an enhanced probability of excimer formation occurring after the exciton has reached the site.  $\beta$  would then be less than unity, with  $1 - \beta$  being the fraction of time the exciton will become trapped due to this increased excimer-forming probability.

In general, an exciton landing on an EFS trap which terminates a sequence of nontrap sites would be expected to lead to excimer fluorescence. It is possible, however, that thermal agitation could cause dissociation to an excited monomer which would subsequently fluoresce. To account for this, the parameter  $d$ , which is the probability that monomer emission results upon trapping, is included for cases B and C.

The boundary conditions for each of the sequences may then be written in general as follows:

Case A

$$F_a(m, 0) = \beta F_a(m, 1) \quad (5a)$$

$$F_a(m, m + 1) = \beta F_a(m, m) \quad (5b)$$

Case B

$$F_b(m, 0) = \beta F_b(m, 1) \quad (6a)$$

$$F_b(m, m + 1) = d \quad (6b)$$

Case C

$$F_c(m, 0) = d \quad (7a)$$

$$F_c(m, m + 1) = d \quad (7b)$$

These boundary conditions may be applied in turn to eq 3 to yield  $F(m, k)$ .

Since all nontrap starting locations are spectroscopically equivalent, the expression for  $F(m, k)$  must be averaged over all starting locations,  $k$ , within the given sequence. This averaging is done by summing the contributions from each monomer site in the sequence and dividing by the number of sites.

$$\begin{aligned} F(m) &= \frac{1}{m} \sum_{k=1}^m F(m, k) \\ &= 1 + \frac{C_1}{m} \sum_{k=1}^m e^{2\gamma k} + \frac{C_2}{m} \sum_{k=1}^m e^{-2\gamma k} \end{aligned} \quad (8)$$

The summations may be evaluated by using

$$\sum_{k=1}^{n-1} z^k = \frac{z^n - z}{z - 1} \quad (9)$$

$F(m)$  is then the probability of eventual monomer emission from an exciton which starts anywhere within a given sequence of  $m$  nontrap sites.

Application of these procedures to case A boundary conditions yields

$$F_a(m) = 1 - \frac{A2(m)[e^{2\gamma(m+1)} - e^{2\gamma}]}{m[e^{2\gamma} - 1]} - \frac{A1(m)[e^{-2\gamma(m+1)} - e^{-2\gamma}]}{m[e^{-2\gamma} - 1]} \quad (10)$$

where

$$A1(m) = \frac{1 - \beta}{2} (\beta e^{2\gamma m} - e^{2\gamma(m+1)} - \beta e^{2\gamma} + 1) / (2\beta \sinh (2\gamma m) - \sinh [2\gamma(m+1)] - \beta^2 \sinh [2\gamma(m-1)]) \quad (11)$$

and

$$A2(m) = \frac{1 - \beta}{1 - \beta e^{2\gamma}} + \left[ \frac{\beta e^{-2\gamma} - 1}{1 - \beta e^{2\gamma}} \right] A1(m) \quad (12)$$

As a check on this expression we will consider limiting values of the parameters. If there is no enhancement of excimer formation at the chain end, i.e., if the boundaries are purely reflecting ( $\beta = 1$ ), eq 10 predicts that  $F_a(m) = 1$ . This is reasonable since, if there are no traps present and if there is also no possibility of additional excimers being formed at the chain ends, the exciton cannot possibly yield anything but monomer emission. Conversely, if both ends are assumed to form excimers with unit efficiency whenever the exciton attempts to hop off the chain ( $\beta = 0$ ), it can easily be shown that the result is identical with that obtained using case C boundary conditions with  $d = 0$ . This is also to be expected since such absorbing boundaries are functionally equivalent to traps in terminating the sequence of monomer sites.

For case B boundary conditions the corresponding expression is

$$F_b(m) = 1 + \frac{d-1}{m} \left[ \frac{e^{2\gamma(m+1)} - e^{2\gamma}}{e^{2\gamma} - 1} \right] - \frac{B1(m)}{2m} \left[ \frac{\cosh (2\gamma m + \gamma) - \cosh (\gamma)}{\sinh (\gamma)} \right] \quad (13)$$

where

$$B1(m) = \frac{(\beta - 1) + (d - 1)(\beta e^{2\gamma m} - e^{2\gamma(m+1)})}{\beta \sinh (2\gamma m) - \sinh [2\gamma(m+1)]} \quad (14)$$

As a check on this relation, we may determine the corresponding expression in limiting situations. If the trap emits only monomer fluorescence ( $d = 1$ ) and the chain end has a purely reflecting character ( $\beta = 1$ ), examination of eq 13 indicates that  $F_b(m) = 1$ , as expected. If only excimer fluorescence comes from the trap ( $d = 0$ ) and the elastic boundary at the chain end is strictly absorbing ( $\beta = 0$ ), the expression reduces to that given by case C when  $d = 0$ .

Finally, for case C boundary conditions

$$F_c(m) = 1 + \frac{(d - 1) \sinh (\gamma m)}{m \cosh [\gamma(m + 1)] \sinh (\gamma)} \quad (15)$$

If only excimer fluorescence comes from the traps ( $d = 0$ ), this equation reduces to the same form as Levinson's<sup>13</sup> eq 5. Conversely, if the traps only emit in the monomer region ( $d = 1$ ), eq 15 predicts the expected result  $F_c(m) = 1$ .

**4. Distribution of Monomer Sequence Lengths.** The probability that the exciton begins on a monomer unit which is part of a run of  $m$  consecutive nontrap units with boundaries of type  $x$  in a chain of length  $L$  will be denoted  $G_x(m, L)$ .

To develop an expression for  $G_x(m, L)$ , we first use a geometric probability distribution to determine the likelihood that the given sequence is found at a specific location on the chain. This geometric probability is then multiplied by the number of ways the sequence can be placed on the chain, yielding the expected number of such sequences in a polymer of length  $L$ . When this value is multiplied by the number of monomer units in the sequence,  $m$ , the resulting expression gives the expected number of monomer segments from the given type of sequence present in the chain. Subsequent division by the total number of segments per chain,  $L$ , yields  $G_x(m, L)$ .

Note that an EFS is assumed to result when the rotational conformation of an adjacent pair of repeat units is in the meso tt conformation, with only minor contributions from other conformational possibilities. This assumption has been made in earlier work<sup>23,24</sup> and is discussed further in the following paper. Since the probability of finding an excimer trap,  $q$ , is proportional to the concentration of such rotational dyads, the important elements are the  $L - 1$  bond dyads between the monomer repeat units rather than the  $L$  monomer units which have been the focus of attention so far.

For case A boundary conditions there are no excimer sites on the chains; thus

$$G_A(L, L) = (1 - q)^{L-1} \quad (16)$$

In case B the sequence could be bounded by a chain end on either its right or left sides; thus,

$$G_B(m, L) = 2(1 - q)^m q \left( \frac{m}{L} \right); \quad m \leq L - 2 \quad (17)$$

where the disposition of the other  $L - 2 - m$  units on the chain has no effect on this probability. For case C the expression is

$$G_C(m, L) = (L - m - 3)q^2(1 - q)^{m+1} \left( \frac{m}{L} \right); \quad m \leq L - 4 \quad (18)$$

where the number of ways that  $m$  contiguous nonexcimer dyads bounded by two excimers could be placed on a polymer chain of length  $L$  is given by  $L - m - 3$ .

**5. Overall Probability of Monomer Emission.** The probabilities of monomer emission from each type of sequence derived in eq 10-15 are combined with the corresponding probabilities for occurrence of the particular sequence in eq 16-18 to yield the overall probability of monomer emission  $M(\alpha, q, L)$

$$M(\alpha, q, L) = \sum_{x=1}^3 \sum_m G_x(m, L) F_x(m) = \sum_{m=1}^L (1 - q)^{L-1} \left[ 1 - \frac{A2(m)(e^{2\gamma(m+1)} - e^{2\gamma})}{m(e^{2\gamma} - 1)} - \frac{A1(m)(e^{-2\gamma(m+1)} - e^{-2\gamma})}{m(e^{-2\gamma} - 1)} \right] + \sum_{m=1}^{L-2} 2(1 - q)^m q \left( \frac{m}{L} \right) \times \left\{ 1 + \frac{d-1}{m} \left[ \frac{e^{2\gamma(m+1)} - e^{2\gamma}}{e^{2\gamma} - 1} \right] - \frac{B1(m)}{2m} \left[ \frac{\cosh (2\gamma m + \gamma) - \cosh (\gamma)}{\sinh (\gamma)} \right] \right\} + \sum_{m=1}^{L-4} (L - m - 3)q^2(1 - q)^{m+1} \left( \frac{m}{L} \right) \left[ 1 + \frac{(d - 1) \sinh (\gamma m)}{m \cosh (\gamma m + \gamma) \sinh (\gamma)} \right] \quad (19)$$

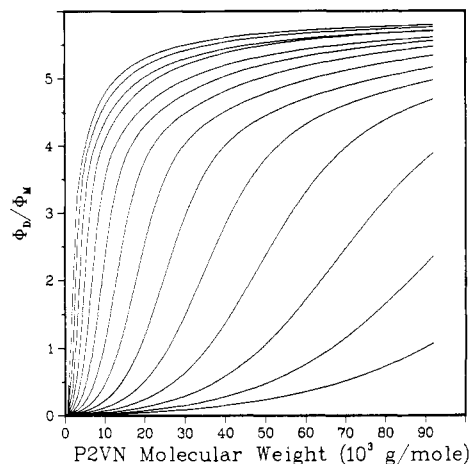


**Figure 1.** Family of predicted curves for various combinations of emission probability ( $\alpha$ ) and trap concentration ( $q$ ) which reproduce the value of  $\phi_D/\phi_M = 5.88$  at a molecular weight of 270 000. In these fits the following parameter values were used:  $\beta = 1$ ,  $d = 0$ ,  $D = 1$ . The best ( $\alpha, q$ ) pair is selected by comparison of the family of curves with experimental  $\phi_D/\phi_M$  data over a range of molecular weights.

**6. Photophysics.** In the analysis presented so far, the emphasis has been on the statistics of the one-dimensional random walk. In order to apply this model to experimental results, it is necessary to adopt a photophysical decay scheme for excimer fluorescence. The most widely used decay scheme has been the one developed by Birks for intermolecular excimer fluorescence.<sup>19</sup> An expression for the photostationary state ratio of excimer to monomer quantum yields for intramolecular excimer fluorescence which is similar to the Birks result may be derived if  $k_{DM}$  is taken to refer to all processes other than monomer decay. This includes energy migration and rotational motion into an excimer-forming geometry.

Some defined quantities that will subsequently be of use are

$$k_M \equiv k_{FM} + k_{IM} \quad (20a)$$

$$k_D \equiv k_{FD} + k_{ID} \quad (20b)$$

$$Q_M \equiv k_{FM}/k_M \quad (20c)$$

$$Q_D \equiv k_{FD}/k_D \quad (20d)$$

Here  $k_M$  and  $k_D$  are the rate constants for monomer and excimer decay by all means except for interconversion between excimer and monomer, and  $Q_M$  and  $Q_D$  are the intrinsic quantum yields for monomer and excimer fluorescence. The rate constants  $k_{FM}$  and  $k_{FD}$  refer to monomer and excimer fluorescence decay, and  $k_{IM}$  and  $k_{ID}$  are the corresponding rates for internal conversion.

The observed monomer quantum yield in the presence of excimers,  $\phi_M$ , may be represented by the following expression when excimer dissociation to excited monomer occurs.

$$\begin{aligned} \phi_M &= \frac{k_{FM}}{k_M + k_{DM}} + \left[ \frac{k_{DM}}{k_M + k_{DM}} \right] \left[ \frac{k_{MD}}{k_D + k_{MD}} \right] \left[ \frac{k_{FM}}{k_M} \right] \\ &= \frac{Q_M k_M}{k_M + k_{DM}} + \left[ 1 - \frac{k_M}{k_M + k_{DM}} \right] \left[ 1 - \frac{k_D}{k_D + k_{MD}} \right] Q_M \end{aligned} \quad (21)$$

The first term accounts for fluorescence from a monomer unit before it has a chance to form an excimer while the second term takes into account the fluorescence contribution from excited monomer units which have been

formed by the dissociation of an excimer complex. The factors in the second term are the probability of excimer formation, the probability that the excimer dissociates to an excited monomer, and the intrinsic monomer quantum yield, respectively.

Note that the ratio  $k_M/(k_M + k_{DM})$  is the probability of eventual radiative or nonradiative emission from the monomer state. It is thus equivalent to  $M(\alpha, q, L)$  of eq 19. The probability of eventual excimer emission from an excimer complex,  $k_D/(k_D + k_{MD})$  is analogously set equal to a quantity  $D$ . Equation 21 may thus be written

$$\phi_M = Q_M M(\alpha, q, L) + [1 - M(\alpha, q, L)][1 - D]Q_M = Q_M(1 - D[1 - M(\alpha, q, L)]) \quad (22)$$

The excimer quantum yield is given by the product of the probability that the excimer is formed and the probability that it subsequently emits fluorescence

$$\phi_D = \left[ \frac{k_{DM}}{k_M + k_{DM}} \right] \left[ \frac{k_{FD}}{k_D + k_{MD}} \right] = Q_D[1 - M(\alpha, q, L)]D \quad (23)$$

Division of eq 23 by eq 22 leads to

$$R \equiv \frac{\phi_D}{\phi_M} = \frac{Q_D}{Q_M} \left[ \frac{D(1 - M)}{1 - D(1 - M)} \right] \quad (24)$$

while addition of eq 22 and 23 yields

$$S \equiv \phi_D + \phi_M = [1 - D(1 - M)]Q_M + D(1 - M)Q_D \quad (25)$$

Combination of eq 24 and 25 gives

$$\frac{Q_D}{Q_M} = \frac{\phi_D}{Q_0 - \phi_M} = \frac{S - \left( \frac{S}{1 + R} \right)}{Q_0 - \left( \frac{S}{1 + R} \right)} \quad (26)$$

where  $Q_0$  is the monomer quantum yield in the absence of excimer formation.

If  $Q_0$  is assumed equal to the total fluorescence quantum yield of a monomeric model compound with the same chromophore concentration as that of the polymer and the value of  $D$  is known, an experimental value of  $M(\alpha, q, L)$  can be determined. The procedure for this determination involves first solving for  $Q_D/Q_M$  in eq 26 and then using that value to solve for  $M(\alpha, q, L)$  in eq 24.

**7. Behavior of Model.** The two variables of interest for characterizing the photophysical properties of the aromatic vinyl polymers are  $\alpha$  and  $q$ , which are contained implicitly in eq 19 and 24. At any particular molecular weight, an infinite number of ( $\alpha, q$ ) pairs will be capable of reproducing the observed  $M(\alpha, q, L)$ . This is demonstrated in Figure 1 in which the molecular weight dependence of the predicted  $\phi_D/\phi_M$  ratio is plotted for several ( $\alpha, q$ ) pairs. Each pair reproduced the value of  $\phi_D/\phi_M = 5.88$  for a P2VN sample of molecular weight 270 000. The top curve has an  $\alpha = 1.56 \times 10^{-3}$  and a  $q = 0.299$ ; the bottom curve has  $\alpha = 1.91 \times 10^{-7}$  and  $q = 0.00552$ . For intermediate curves,  $\alpha$  is equal to half the value for the curve directly above. The values of  $q$  decline in a less orderly fashion from the top to the bottom of the plot.

Only one ( $\alpha, q$ ) pair, however, will be capable of reproducing the  $M(\alpha, q, L)$  at all the molecular weights. Thus, if experimental quantum yield data on  $\phi_M$  and  $\phi_D$  are available for several molecular weights,  $M(\alpha, q, L)$  may be calculated and a Regula-Falsi regression analysis may be used to extract numerical values for  $q$  and  $\alpha$ .

The magnitude of  $\phi_D/\phi_M$  predicted with eq 24 also depends on the magnitudes of the parameters  $\beta$ ,  $d$ , and  $D$ .

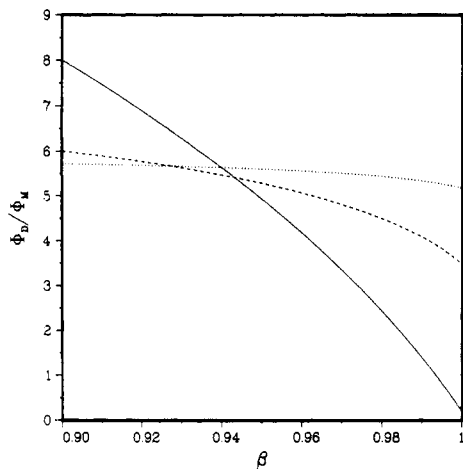


**Figure 2.** Dependence of fluorescence ratio calculated with eq 24 on the parameter  $\beta$ . For these curves  $q = 0.1033$ ,  $\alpha = 1.185 \times 10^{-4}$ ,  $d = 0$ , and  $D = 1$ . The P2VN molecular weights considered were (—) 2500, (---) 10000, and (···) 60000.

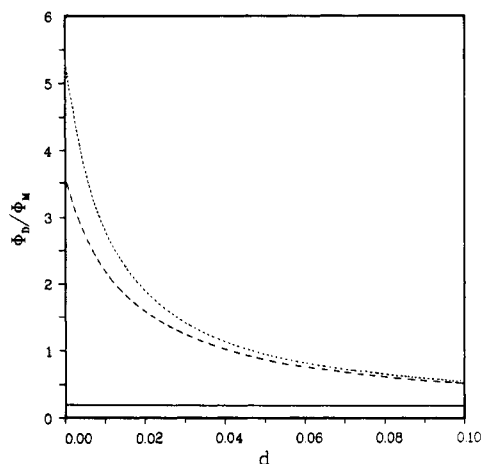


**Figure 3.** Dependence of fluorescence ratio calculated with eq 24 on the parameter  $d$ . For these curves  $q = 0.1033$ ,  $\alpha = 1.185 \times 10^{-4}$ ,  $\beta = 1$ , and  $D = 1$ . The P2VN molecular weights considered were (—) 2500, (---) 10000, and (···) 60000.

As  $\beta$  and  $d$  are varied, the fluorescence ratios predicted with eq 24 vary as shown in Figures 2 and 3, respectively. The values of  $d$  and  $D$  will be 0 and 1, respectively, at temperatures which are low enough to prevent thermal dissociation of an excimer to excited- and ground-state monomers. Since this is the region in which the experimental data considered in this paper lie, those values will be used for subsequent analysis. In addition,  $\beta$  is taken to be unity for the data reported in this work.

### Experimental Section

A series of P2VN samples with various molecular weights was prepared by free radical polymerization initiated by azobis(isobutyronitrile) (AIBN). The molecular weight was controlled by varying the AIBN concentration and the ratio of carbon tetrachloride to toluene in the solvent. The 2-vinylnaphthalene monomer was purchased from Aldrich and purified by vacuum sublimation. The AIBN initiator was also purchased from Aldrich and purified by recrystallization in methanol. Distillation was used to purify the toluene and carbon tetrachloride solvents, which were obtained from Fisher. The polymer was purified by multiple precipitations from toluene using Baker Photorex methanol as the nonsolvent.

The polymer molecular weight was determined by intrinsic viscosity measurements in toluene at 293 K and by gel phase chromatography using a Waters Model 244 liquid chromatograph with six  $\mu$ -Styragel columns.

All fluorescence samples were at a concentration of  $10^{-4}$  M in naphthalene repeat units. Oxygen was removed by applying four

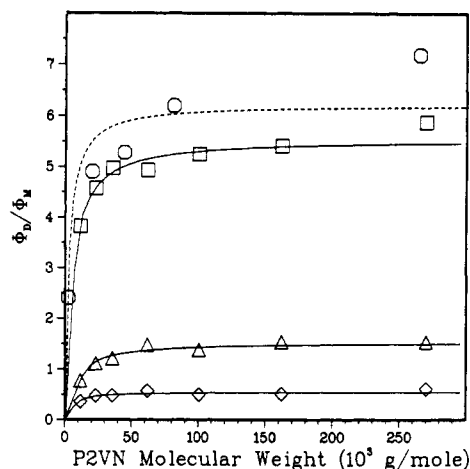


**Figure 4.** Molecular weight dependence of  $\phi_D/\phi_M$ . Data were obtained from Nishijima<sup>8</sup> [( $\diamond$ ) 203 K, ( $\Delta$ ) 223 K, ( $\square$ ) 253 K] and from this work [( $\circ$ ) 298 K]. The data from this work should be multiplied by 2. The smooth curves are the predictions of the model for the best fit to the data.

**Table I**  
Best Fits for the Random Walk Model

$T, K$	$\Delta^2$	$\alpha \times 10^4$ <sup>d</sup>	$q$ <sup>d</sup>	$q_{sim}$ <sup>e</sup>	$q/q_{sim}$
298 <sup>a</sup>	5.77	33.3	0.197	0.0135	14.6
298 <sup>b</sup>	17.2	33.3	0.198	0.0135	14.7
253 <sup>c</sup>	0.206	11.2	0.0823	0.0082	10.0
223 <sup>c</sup>	0.179	3.02	0.0204	0.0051	4.0
203 <sup>c</sup>	0.00963	7.46	0.0142	0.0035	4.1

<sup>a</sup> Data from this work: 2-methyltetrahydrofuran solution. <sup>b</sup> Data from this work: toluene solution. <sup>c</sup> Data from ref 8. <sup>d</sup> In all fits  $Q_D/Q_M = 0.6$ ,  $\beta = 1$ ,  $d = 0$ , and  $D = 1$ . <sup>e</sup> The value listed is the tt meso concentration predicted using rotational isomeric state theory and a Monte Carlo simulation divided by 2 to account approximately for the expected reduction in stability of excimer-forming sites in which the axes form a  $60^\circ$  angle.

freeze-pump-thaw cycles and then sealing off the sample at  $10^{-4}$  torr in 0.5-in. cylindrical quartz tubes. The spectrometer, data acquisition system, and data analysis routines have been described previously.<sup>24</sup>

### Results

**1. Fit of Experimental Data.** The one-dimensional random walk model has been applied to the analysis of two sets of data on the molecular weight dependence of P2VN. The first set, obtained in this study, is for P2VN in both toluene and 2-methyltetrahydrofuran (MTHF) solution at 298 K. The second set, obtained by Nishijima,<sup>8</sup> is for P2VN in MTHF at 253, 223, and 203 K.

The experimental  $\phi_D/\phi_M$  results for these data, presented in Figure 4, were analyzed under the assumption that the molecular weight distribution is given by the Flory-Schultz expression.<sup>25</sup> The smooth curves represent the best fits of the one-dimensional random walk model to the results. The values of  $q$  and  $\alpha$  corresponding to the best fits are given in Table I.

The criterion for selection of the best fit was the minimization of the sum of the squares of the differences between the predicted and experimental values of  $\phi_D/\phi_M$ , termed  $\Delta^2$  in Table I. The relative variation of this residual with  $q$  is plotted for Nishijima's data in Figure 5. In this figure,  $q_0$  refers to the value from the best fit. The corresponding plot for  $\log \alpha$  is given in Figure 6. As can be seen, the value for  $q$  is much more precisely defined than is  $\alpha$ . The relative shallowness of the minima is due to the small number of data points which lie on the sharply in-

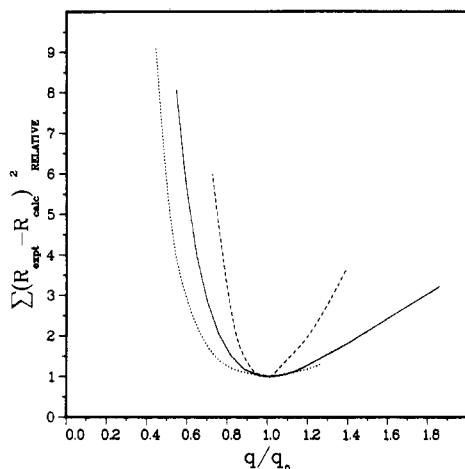


**Figure 5.** Sum of the squares of the deviations between the experimental and predicted  $\phi_D/\phi_M$  divided by the corresponding quantity for the best fit as a function of  $q/q_0$ , where  $q_0$  is the trap concentration at the best fit. The curves refer to Nishijima's data:<sup>8</sup> (...) 203 K; (---) 223 K; (—) 253 K.

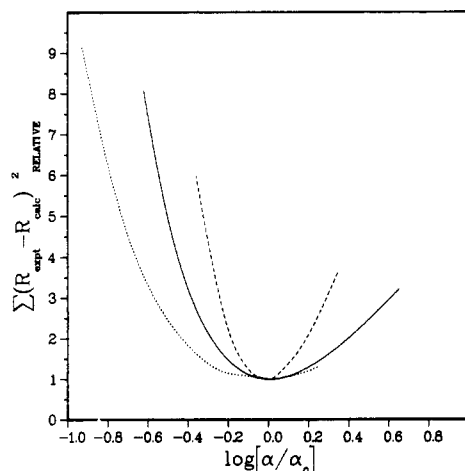


**Figure 6.** Sum of the squares of the deviations between the experimental and predicted  $\phi_D/\phi_M$  divided by the corresponding quantity for the best fit as a function of  $\log(\alpha/\alpha_0)$ , where  $\alpha_0$  is the emission probability at the best fit. The curves refer to Nishijima's data:<sup>8</sup> (...) 203 K; (---) 223 K; (—) 253 K.

creasing portions of the curves of Figure 4. As seen in Figure 1, the shape of the  $\phi_D/\phi_M$  curve at low molecular weight and the molecular weight at which the curve levels out are the major factors which discriminate among the possible  $(\alpha, q)$  pairs.

It is clear from Figure 4 and the  $\Delta^2$  values of Table I that the predicted  $\phi_D/\phi_M$  agrees quite well with the experimental points at temperatures of 203 and 223 K. At higher temperatures, however, the fit is not as good at the highest molecular weights.

In order to determine whether the values of  $q$  and  $\alpha$  which give the best fit to the data are reasonable and whether the deviation of the model from the experimental results at high molecular weight and temperature is significant, it is necessary to have independent estimates of  $q$  and  $\alpha$ . These are obtained in the following sections.

**2. Estimation of Excimer-Forming Site Population  $q$ .** An EFS in a polymer in dilute solution may be formed by two processes.<sup>24</sup> First, there will be an equilibrium concentration of preformed excimer sites which consist mainly of meso tt dyads. In addition, there are sites which are formed during the residence time of the exciton at a given location by relative motion of adjacent polymer segments. At low temperatures, the enhancement of the

EFS concentration by the second process will be minimal. In that case,  $q$  may be estimated from the probability of occurrence of preformed meso tt dyads.

Such calculations require knowledge of the conformational energy as a function of bond rotation angle.<sup>26</sup> When this work was begun, such data were available for 2,4-bis(2-naphthyl)pentane (DNPE)<sup>27</sup> but not for poly(2-vinylnaphthalene). However, based upon molecular models, the conformational energies for P2VN were expected to be similar to those for polystyrene,<sup>28</sup> for which the rotational isomeric state calculations had been performed.<sup>29</sup> Recent calculations on steric energies in poly(1-vinylnaphthalene) and P2VN by Seki et al. have confirmed the similarities between PS and P2VN.<sup>30</sup> Thus, the calculations reported in this work, which are based on the PS energy maps,<sup>29</sup> should be valid for P2VN.

A Monte Carlo analysis was used to estimate the equilibrium concentration of tt meso dyads at 203, 223, 253, and 298 K. The first step in this analysis was the use of Yoon's<sup>29</sup> PS statistical weights to calculate the trans conditional probabilities  $P(t/t, \text{meso})$ ,  $P(t/t, \text{racemic})$ ,  $P(t/g, \text{meso})$ , and  $P(t/g, \text{racemic})$  and the corresponding gauche probabilities at each temperature. These probabilities were then used in constructing 3000, 50% meso chains of length 20.

From Table I it is seen that the ratio  $q/q_{\text{sim}}$  is small at 203 K and rises with temperature. This is to be expected if the enhancement of the effective EFS concentration occurs by the thermally activated process of segmental motion.

**3. Estimation of  $\alpha$ .** The estimation of  $\alpha$ , the probability of monomer emission rather than exciton hopping, requires knowledge of both the rate of fluorescence decay and the rate of energy transfer. Information on the rate of fluorescence decay or its inverse, the fluorescence lifetime, is readily available. The rate of energy transfer, however, depends upon the relative distance and orientation of the energy-donating and -accepting chromophores. To evaluate this rate, the relative positions of the chromophores in the polymer must be determined. A Monte Carlo simulation was used to accomplish this.

In this simulation the pendant chromophores were positioned on a tetrahedral lattice by using Yoon's<sup>29</sup> probabilities for polymer dyad conformations in PS at 300 K and a random number generator to place successive segments of the polymer. Each point of the diamond lattice used for polymer placement has four vectors emanating from it, with the angle between any pair of vectors being  $109.47^\circ$ . If the vectors are denoted **a**, **b**, **c**, and **d**, the three-space coordinates of the bonds may be described by

$$\mathbf{a} = (3, 0, 0) \quad (27a)$$

$$\mathbf{b} = (-1, 0, 2) \quad (27b)$$

$$\mathbf{c} = (-1, 1, -1) \quad (27c)$$

and

$$\mathbf{d} = (-1, -1, -1) \quad (27d)$$

Each of the above should be multiplied by the vector  $(1/3, (2/3)^{1/2}, 2^{1/2}/3)$  to yield the actual displacement of each vector in three-dimensional Cartesian coordinates. The coordinates are right handed when the order is taken to be **a**, **b**, **c**, and then **d**.

The direction of a given backbone bond is determined from the directions of the two preceding bonds on the chain and the rotational conformation of the dyad to which the bond belongs. If the conformation is trans, the bond will have the same tetrahedral vector as the next to the

Table II  
Results of Monte Carlo Modeling of the Energy Migration Rate

T, K	$\sigma^a$	$\Delta E^b$	$P(m)^c$	$T^d$			$k_E^e \times 10^{-9}, s^{-1}$
				$s = 1$	$s = 2$	$s = 3$	
300	3.9	2.4	0.3	3.76	0.255	0.018	4.04
	3.9	2.4	0.5	7.10	0.423	0.027	7.55
	5.0	0.9	0.3	4.73	0.332	0.022	5.09
	5.0	0.9	0.5	8.45	0.502	0.033	9.00
203	3.9	2.4	0.3	1.53	0.103	0.005	1.64
	3.9	2.4	0.5	2.62	0.140	0.008	2.77
	5.0	0.9	0.3	3.45	0.245	0.016	3.77
	5.0	0.9	0.5	5.88	0.342	0.023	6.25

<sup>a</sup>  $\sigma$  is the distance, in Å, at which the solvent shields polymer-polymer interactions. Yoon<sup>29</sup> concludes that a value between 3.9 and 5 Å is reasonable. <sup>b</sup>  $\Delta E = E_{tt,m} - E_{tg,m}$  (kcal/mol), where  $E_{tt,m}$  and  $E_{tg,m}$  are the conformational energies of the tt,meso and tg,meso dyads as reported in ref 29. <sup>c</sup> Fraction of meso dyads. <sup>d</sup> Relative number of transfers to the  $s$ th nearest neighbor. <sup>e</sup> Energy transfer rate constant.

last bond considered. For example, if the first two bonds were along the "a" and "b" tetrahedral vectors the third would be along the "a" vector for a trans conformation.

Since substituents are considered to be perpendicular to the local direction of the polymer backbone,<sup>29</sup> there are only two possible relative orientations which could be assumed by naphthyl rings in an adjacent arrangement. They can be oriented either with their long axes pointing in the same direction or with their axes making a 60° angle. Energy transfer should be possible in both configurations.

Simulations were run on chains consisting of 20 repeat units, as well as on shorter chains. Excluded volume effects were accounted for by elimination of all conformational sequences resulting in backbone or pendant group carbon overlap. In order to obtain an ensemble of 3000 valid chains, between 6000 and 20 000 chains had to be generated. For each valid chain, the rate of energy transfer from a unit on the end of the chain to every other unit on the chain was then calculated by assuming solely dipole-dipole resonance interactions. The dependence of the transfer rate on the relative distances and orientation of the naphthyl groups is given by

$$k_{\text{transfer}} = \frac{3\kappa^2}{2\tau} \left( \frac{R_0}{r} \right)^6 \quad (28)$$

where  $R_0$ ,  $r$ , and  $\tau$  are the same as defined for eq 1 and  $\kappa^2$  takes account of the relative orientation of the donor and acceptor. If the optical dipoles are parallel,  $\kappa^2 = 1$ ; if they make a 60° angle,  $\kappa^2 = 1/4$ ; and if they are randomly oriented,  $\kappa^2$  averages to  $2/3$ . For 2-methylnaphthalene the Förster radius is 11.75 Å and the unperturbed lifetime in cyclohexane is 60 ns.<sup>31</sup> These values are assumed to also apply for P2VN. Since higher multipole interactions and electronic exchange transfer will also contribute to energy transfer, the transfer rate calculated by this routine should provide a lower bound to the actual transfer rate.

The overall transfer rate constants reported in Table II were generated by summing the rates of transfer from the terminal unit to every other unit except for the neighboring unit when the two chromophores are in an excimer-forming configuration. The result is multiplied by 2 to account for the possibility that the chain continues on the other side of the terminal unit. Two possible ratios of tacticities were considered in modeling the atactic samples considered in this investigation: 50% isotactic and 30% isotactic. The former is probably closer to the true value.<sup>32</sup> In Table II average rates of transfer are given for the statistical weights reported by Yoon et al.,<sup>29</sup> using each tacticity for two different values for the solvent shielding distance,  $\sigma$ . It is interesting to note that even though the next nearest

neighbors have twice the probability of being oriented such that energy transfer is possible, the closeness of the nearest neighbors and the short range (11.75 Å) of the dipole-dipole transfer mechanism ensures that the majority of the transfers in P2VN will be to nearest neighbors whose long axes form a 60° angle with the long axis of the first chromophore. The average rate of transfer to nearest neighbors with parallel naphthalene axes (EFS) was found to be 1.6 times larger than the calculated migration rate.

As noted in eq 2  $\alpha$  is the probability at any step in the random walk that monomer decay takes place by radiative or nonradiative emission. Since the only other possible option for the exciton is to migrate,  $\alpha$  may be written as

$$\alpha = k_M / (k_M + k_E) \quad (29)$$

where  $k_M$  is defined by eq 20a and  $k_E$  is the rate constant for energy transfer. If  $k_M$  is taken to be the reciprocal of the monomer lifetime, 60 ns, and  $k_E$  is taken to be the simulated energy migration rate,  $\alpha$  is estimated to lie between  $1.8 \times 10^{-3}$  and  $2.5 \times 10^{-3}$ . This agrees reasonably well with the values of  $\alpha$  determined from the random walk model.

## Discussion

From examination of Tables I and II and Figure 4, it is clear that this model is capable of explaining the observed molecular weight dependence of excimer fluorescence with physical parameters which are reasonable. There are, however, deviations between experiment and theory. Specifically,  $\phi_D/\phi_M$  at highest molecular weight shows an increasing deviation from the predicted value as the temperature is raised. In addition, the trap concentrations derived are higher than the equilibrium concentrations predicted from rotational isomeric state calculations, with the deviation increasing as the temperature is raised.

As noted earlier, a basic assumption of the modeling effort has been that the EFS traps are immobile. To test this assumption, it is of interest to compare the rates of energy migration, as given in Table II, with literature data on the rate of segmental rotation. In a recent publication, Friedrich et al.<sup>33</sup> determined the rate of segmental motion in polystyrene at temperatures between 273 and 363 K by electron spin resonance. At 300 K they determined that the rate constant for segmental motion,  $k_{\text{rot}}$ , was equal to  $4.2 \times 10^9 s^{-1}$ , which is comparable to the value of the energy transfer rate of about  $7.6 \times 10^9 s^{-1}$ , as given in Table II for 50% meso dyads. Thus, enhancement of the effective EFS concentration by segmental motion is expected to be extensive.



In that same work, the correlation times for the lowest temperatures were fit to the Arrhenius relation

$$k_{\text{rot}}^{-1} = \tau_{\text{rot}} = 2.46 \times 10^{-13} \exp[4100/RT] \quad (30)$$

where  $R = 1.986 \text{ cal}/(\text{mol K})$ . If eq 30 also holds for temperatures less than 272 K, we estimate the rate of segmental motion at 203 K to be  $1.6 \times 10^8 \text{ s}^{-1}$ . From Table II, we see that the energy transfer rate at 203 K is  $277 \times 10^9 \text{ s}^{-1}$ , or 17 times faster than the extrapolated rate of segmental motion. The closer agreement between  $q$  and  $q_{\text{sim}}$  is consistent with this.

In view of the importance of segmental motion to the photophysical processes at high temperatures, the phenomenon bears further examination. The most direct effect of segmental mobility would be to cause formation of an EFS at the location of the exciton after the exciton has arrived at the site. This mechanism, which has been examined in a separate study,<sup>24</sup> will serve to increase the effective EFS concentration above the value predicted by equilibrium rotational isomeric state calculations.

Another effect of segmental motion occurring during the energy migration process is that the character of a site may change from a nontrap at the first sampling to a trap at subsequent sampling. The change of status of a location on subsequent sampling is effectively the same as if the random walker were to sample a new location rather than to resample a previous location. The effect of such changes in site identity on the derived parameters will be to raise the values of the predicted  $q$  and  $\alpha$ . This process is expected to be less important than the related enhancement of the trap concentration by excimer formation after an exciton has arrived at the site. This is due to the relatively low equilibrium concentration of meso dyads in the trans,trans conformation.

It is not possible to predict the extent of the enhancement of the EFS concentration due to segmental motion. Nevertheless, it is possible to minimize its influence by examining the aromatic vinyl polymer at low temperature in solution, as was done in this study, or in a rubbery matrix of a second polymer, as in the following paper.<sup>34</sup>

It is also of interest to reexamine the assumption of strict one-dimensional transfer among adjacent units on the polymer chain. It has been shown that the overwhelming majority of transfers to nearby units are to the nearest neighbors. What has not been addressed is the possibility of the polymer looping back such that units in distant positions on the chain come into close proximity. The occurrence of such loops will be minimized by examining the polymer in a good solvent which provides the maximum swelling for isolated polymer chains. Nevertheless, even small amounts of across-loop hops will cause the system to behave in a quasi-one-dimensional manner<sup>35,36</sup> rather than the strict one-dimensionality assumed here. Since the number of distinct sites sampled in  $n$  hops goes as  $n^{1/2}$  for a strictly one-dimensional process and as  $n$  for the first few steps after an across-loop hop in a quasi-one-dimensional process, the calculated concentration of traps should be very sensitive to the dimensionality of the energy transfer process.

As a final point, we note that it has been suggested that the molecular weight dependence of the excimer-to-monomer fluorescence ratio is due solely to the chain ends having a higher probability of attaining an excimer conformation, due to their greater mobility.<sup>1,8</sup> Variation in the  $\beta$  parameter may be included to account for this effect, albeit in a somewhat ad hoc manner. A lower limit for the value of  $\beta$  is estimated by comparing  $\beta\beta\text{DNP}$  fluorescence data to that of P2VN. The estimation procedure involves

first determining the effective concentration of excimer sites,  $q$ , for the highest molecular weight polymer assuming  $\beta = 1$ . The model with this value of  $q$  is applied to  $\beta\beta\text{DNP}$ . The value of  $\beta$  is then lowered until the observed fluorescence is reproduced. This value of  $\beta$  is applied to the polymer samples and a new value of  $q$  is determined for that value of  $\beta$ . This value of  $q$  is fitted with a new  $\beta$  value to reproduce the  $\beta\beta\text{DNP}$  results and the procedure is repeated until it converges. When this procedure was applied to the Nishijima data, values of  $1 - \beta$  very close to zero were obtained: (253 K,  $1.70 \times 10^{-3}$ ; 223 K,  $4.39 \times 10^{-4}$ ; 203 K,  $3.79 \times 10^{-4}$ ). Thus, enhancement of mobility at chain ends is not an important consideration for this model.

## Summary

A one-dimensional random walk model has been developed to explain the molecular weight dependence of excimer formation in the aromatic vinyl polymers. This model has been applied to the photophysical behavior of poly(2-vinylnaphthalene) in dilute solution. Good agreement between the model and the experiment was observed, provided that the temperature and, hence, the segmental rotation rate, was low enough. The success of the model provides support for the existence of singlet energy migration in the aromatic vinyl polymers.

**Acknowledgment.** This work was supported partially by the Institute of Energy Studies at Stanford University and partially by the NSF-MRL Program through the Center for Materials Research at Stanford.

## References and Notes

- (1) MacCallum, J. R. *Eur. Polym. J.* **1980**, *17*, 209.
- (2) Klöpffer, W. *Ann. N.Y. Acad. Sci.* **1981**, *366*, 373.
- (3) Basile, L. J.; Weinreb, A. *J. Chem. Phys.* **1960**, *33*, 1028.
- (4) Heisel, F.; Laustriat, G. *J. Chem. Phys.* **1969**, *66*, 1881.
- (5) Ishii, T.; Handa, T.; Mori, S.; Utena, Y. *Rep. Prog. Polym. Phys. Jpn.* **1978**, *21*, 361.
- (6) North, A. M.; Treadaway, M. F. *Eur. Polym. J.* **1973**, *9*, 609.
- (7) Lindsell, W. E.; Robertson, P. C.; Soutar, I. *Eur. Polym. J.* **1981**, *17*, 203.
- (8) Nishijima, Y.; Mitani, K.; Katayama, S.; Yamamoto, M. *Rep. Prog. Polym. Phys. Jpn.* **1970**, *13*, 421.
- (9) Ito, S.; Yamamoto, M.; Nishijima, Y. *Rep. Prog. Polym. Phys. Jpn.* **1976**, *19*, 421.
- (10) Ito, S.; Yamamoto, M.; Nishijima, Y. *Rep. Prog. Polym. Phys. Jpn.* **1978**, *21*, 393.
- (11) Barber, M. N.; Ninham, B. W. "Random and Restricted Walks: Theory and Applications"; Gordon and Breach: New York, 1970.
- (12) Rosenstock, H. B. *J. Soc. Ind. Appl. Math.* **1961**, *9*, 169.
- (13) Levinson, N. J. *Soc. Ind. Appl. Math.* **1962**, *10*, 442.
- (14) Klöpffer, W. *J. Chem. Phys.* **1969**, *50*, 2337.
- (15) Rudemo, M. *SIAM J. Appl. Math.* **1966**, *14*, 1293.
- (16) Dale, R. E.; Eisinger, J. *Proc. Natl. Acad. Sci. U.S.A.* **1976**, *73*, 271.
- (17) Ishii, T.; Matsunaga, S.; Handa, T. *Makromol. Chem.* **1976**, *177*, 283.
- (18) Boudevska, H.; Brutchkov, C.; Astrug, A. *Makromol. Chem.* **1979**, *180*, 1113.
- (19) Birks, J. B. "Photophysics of Aromatic Molecules"; Interscience: London, 1970.
- (20) Ishii, T.; Handa, T.; Matsunaga, S. *Macromolecules* **1978**, *11*, 40.
- (21) Webber, S. E.; Avots-Avotins, P. E.; Deumie, M. *Macromolecules* **1981**, *14*, 105.
- (22) Zumofen, G.; Blumen, A. *Chem. Phys. Lett.* **1981**, *78*, 131.
- (23) Frank, C. W.; Gashgari, M. A. *Ann. N.Y. Acad. Sci.* **1981**, *366*, 387.
- (24) Fitzgibbon, P. D.; Frank, C. W. *Macromolecules* **1981**, *14*, 1650.
- (25) Flory, P. J. "Principles of Polymer Chemistry"; Cornell University Press: Ithaca, N.Y., 1953.
- (26) Flory, P. J. "Statistical Mechanics of Chain Molecules"; Interscience: New York, 1969.
- (27) Nishijima, Y.; Yamamoto, M. *Polym. Prepr., Am. Chem. Soc., Div. Polym. Sci.* **1979**, *20*, 391.



- (28) Yoon, D. Y., private communication.
- (29) Yoon, D. Y.; Sundararajan, P. R.; Flory, P. J. *Macromolecules* 1975, 8, 776.
- (30) Seki, K.; Ichimura, Y.; Imamura, Y. *Macromolecules* 1981, 14, 1831.
- (31) Berlman, I. B. "Energy Transfer Parameters of Aromatic Compounds"; Academic Press: New York, 1973.
- (32) Bovey, F. A., private communication.
- (33) Friedrich, C.; Laupretre, F.; Noel, C.; Monnerie, L. *Macromolecules* 1981, 14, 1119.
- (34) Gelles, R.; Frank, C. W. *Macromolecules*, part 2, following paper in this issue.
- (35) Wieting, R. D.; Fayer, M. D.; Dlott, D. D. *J. Chem. Phys.* 1978, 69, 1996.
- (36) Dlott, D. D.; Fayer, M. D.; Wieting, R. D. *J. Chem. Phys.* 1978, 69, 2752.

## Energy Migration in the Aromatic Vinyl Polymers. 2. Miscible Blends of Polystyrene with Poly(vinyl methyl ether)

Richard Gelles and Curtis W. Frank\*

Department of Chemical Engineering, Stanford University, Stanford, California 94305.  
Received October 8, 1981

**ABSTRACT:** Excimer fluorescence has been used to study the conformational properties of and energy migration in polystyrene (PS) dispersed at low concentration in miscible blends with poly(vinyl methyl ether) (PVME). Fluorescence spectra of monodisperse PS samples with molecular weights ranging from 2200 to 390 000 were taken at temperatures between 286 and 323 K and analyzed with the one-dimensional random walk model developed by Fitzgibbon.<sup>1</sup> The concentration of excimer-forming sites (EFS) is assumed equal to the fraction of trans,trans meso dyads obtained from rotational isomeric state calculations on chains containing 45% meso dyads. The molecular weight dependence of the ratio of excimer to monomer emission intensities is interpreted in terms of a one-dimensional random walk below 303 K. Slight deviation between the model predictions and experimental data above 303 K is consistent with a decrease in the size of the polystyrene coil caused by unfavorable thermodynamic interactions as the blend approaches the lower critical solution temperature.

### Introduction

In recent years, there has been considerable interest in the photophysics of excimer formation and in energy migration in the aromatic vinyl polymers. In spite of claims to the contrary,<sup>2</sup> there is strong evidence for the existence of singlet energy migration, as reviewed by several authors.<sup>3-5</sup> It should be noted that singlet energy migration must be included in the analysis to explain the results presented in this work.

In the preceding paper of this series, referred to as paper 1, energy migration in an isolated polymer chain was treated as a one-dimensional random walk of the electronic excitation between adjacent pendant chromophores.<sup>1</sup> At each step in the walk, the excitation can be lost radiatively or nonradiatively from an isolated excited chromophore or "monomer". Alternately, the excitation can be trapped at an excimer-forming site (EFS) composed of two adjacent chromophores, leading to radiative or nonradiative emission from the excimer. This approach has been proposed to explain the molecular weight dependence of the ratio of excimer to monomer emission intensities for isolated extended chains.<sup>1</sup>

The purpose of this work is to test the one-dimensional energy migration model quantitatively using a well-characterized system and in so doing to demonstrate how the technique of excimer fluorescence can be used to study conformational properties of polymers. Several criteria must be satisfied, however, before the model may be applied. First, the fluorescent guest polymer must be dispersed at sufficiently high dilution to eliminate both intermolecular excimer sites formed between chromophores on different chains and intermolecular energy migration. Second, the solvent or host matrix must be sufficiently good thermodynamically to minimize intramolecular interaction between aromatic rings on remote repeat units of the guest. Finally, the rate of segmental motion must be much slower than the rate of energy migration, so that excimer-forming sites are immobile and rotational sampling may be ignored. In solution studies such as those

analyzed in the preceding paper it is possible that this final requirement is not met at high temperatures.

All of the necessary specifications are met, however, by the physical blend of polystyrene with poly(vinyl methyl ether). Film casting from toluene has been shown by a variety of experimental techniques<sup>6-10</sup> to lead to apparently miscible systems; thus, low-concentration blends should contain isolated polystyrene chains. In addition, the low glass transition temperature of PVME (245 K) ensures that all low-concentration blends studied will be in the rubbery state. As a result, the conformational population of the polystyrene chains may be assumed to be in equilibrium. Since conformational energy maps exist for polystyrene<sup>11-13</sup> rotational isomeric state calculations of the equilibrium dyad population may be made. Finally, the rotational sampling rate is expected to be inhibited strongly relative to other studies<sup>14-16</sup> in which polystyrene has been examined in solution.

### Experimental Section

Polystyrene samples of molecular weights 2200, 4000, 9000, 17 500, 35 000, 100 000, 233 000, and 390 000 were obtained from Pressure Chemical Co.; they have polydispersities less than or equal to 1.06. They were purified by multiple precipitation from toluene into methanol. The PVME is the GAF Gantrez M-574 product, which has a molecular weight of 44 600 as determined from its intrinsic viscosity in benzene at 303 K. Because of its low glass transition temperature, a special purification technique had to be developed for the PVME. One gram of activated carbon (Norit) per gram of polymer was added to a 0.06 g/mL solution of PVME in toluene. These solutions were shaken vigorously for 3 days, after which the carbon was removed by filtration. This procedure reduced fluorescent impurities in the PVME by a factor of 10.

Solid films, 10  $\mu$ m thick, all at a concentration of 5% by weight of PS, were prepared by casting from toluene solution onto sapphire disks at room temperature. Preliminary concentration studies show that at this concentration, the PS chains are isolated. The films were then dried under vacuum at 323 K for at least 4 days to ensure removal of the casting solvent. No evidence of residual solvent was found from the fluorescence spectra of neat